Numerical comparison of blast waves generated by cylindrical explosive charges with varying shapes and materials

Robert Panowicz, Michał Trypolin, Marcin Konarzewski

Katedra Mechaniki i Informatyki Stosowanej
Wojskowa Akademia Techniczna
Gen. Sylwestra Kaliskiego 2, 00-908 Warsaw, Poland
e-mail: robert.panowicz@wat.edu.pl, michal.trypolin@wat.edu.pl,
marcin.konarzewski@wat.edu.pl

A significant influence of explosive charge geometry is frequently observed during experimental testing. In this paper, the effect of explosive charge shape, along with its material properties, on the generated blast waves is studied. The FEM analysis was conducted for six different explosive materials and three different cylindrical shapes, with geometrical proportions of length L to diameter D varying between 2, 1 and 0.25 and constant charge mass. We found that the blast wave generated by detonation is susceptible to shape changes. However, the different explosive materials were influenced by the charge shape in almost the same way, with only insignificant differences resulting from the material properties.

Keywords: blast wave, FEM, ALE.

1. Introduction

In most tests of blast waves generated by explosive detonations and effects of these waves on structures, cylindrical explosive charges are used. This mainly results from the fact that such charges can be easily manufactured. It is frequently assumed that for sufficiently long distances, a blast wave shape caused by cylindrical charge will not be much different from a blast wave generated by a spherical charge.

During experimental tests of shaped blast wave deflectors impacted by blast waves generated by cylindrical explosives, a significant influence of the shape at a medium distance on the test results was observed. Therefore, we decided to study the influence of an explosive charge shape and its parameters on the resulting blast waves for different explosive materials.

For this study, a fluid-structure interaction (FSI)-arbitrary Lagrangian-Eulerian (ALE) coupled method was chosen, similar to the method used in [1] and described in greater detail in [6]. This method is widely used in blast calculations because it is much less prone to failure due to large mesh distortions caused by the explosion.

In this study, the effects of chemical reactions inside the explosive material as well as the processes forming on the front of the blast wave were omitted, to allow using a programmed burn model [2]. Therefore, the front of the wave moves with constant velocity and produces the strong nonlinearity of surface. Due to this fact, only the elements that were already subjected to the wave at a given time can be investigated. The values of pressure, energy (temperature) and density in the elements located at the front of the wave are equal to the values at the Chapman-Jouguet point. This method allows using increased finite-element mesh density, which enables longer time steps (without compromising the accuracy of the results).

The cited article [1] did not include variable shapes and materials, so this paper will aim to expand the topic by including those variables for greater understanding of the numerical simulations of blast waves in preparation for use in other, more advanced and in-depth studies.

2. Mathematical and numerical model

The Jones-Wilkins-Lee (JWL) equation [3, 4] was used to assess the products of detonation:

$$p = A\left(1 - \frac{\omega}{R_1 V}\right)^{-R_1 V} + B\left(1 - \frac{\omega}{R_2 V}\right)^{-R_2 V} + \omega\rho E, \tag{1}$$

where $V = \rho_0/\rho$, ρ_0 – initial density, ρ – density of detonation products, A, B, R_1, R_2, ω – constants.

The air was described using the Mie-Grüneisen equation [4]:

$$p = p_0 + \gamma\rho E, \tag{2}$$

where p – pressure, p_0 – initial pressure, γ – Grüneisen coefficient, ρ – density, E – internal energy.

The values used in this equation are: $\gamma = 1.4$, $\rho = 1.185$ kg/m^3 and $p_0 = 1013$ hPa [3]. The remaining parameters used in the calculations are presented in Tables 1 and 2.

Table 1. JWL equation constants [3].

Material	Parameter				
	A	B	R_1	R_2	ω
	[GPa]	[GPa]	[–]	[–]	[–]
TNT	373.8	3.747	4.15	0.9	0.35
HMX	778.3	7.071	4.2	1	0.3
Comp. B	524.2	7.7678	4.2	1.1	0.34
PETN	617	16.926	4.4	1.2	0.25
Semtex 10	609.8	12.95	4.5	1.4	0.25
Semtex A1	609.8	12.95	4.5	1.4	0.25

Table 2. Material parameters [3].

Material	Parameter			
	ρ_0	D	p_{CJ}	ρ_{CJ}
	[kg/m^3]	[m/s]	[GPa]	[kg/m^3]
TNT	1630	6930	21	2230
HMX	1890	9110	42	2621
Comp. B	1717	7980	29.5	1770
PETN	1770	8300	33.5	2440
Semtex 10	1530	7486	21.7	2165
Semtex A1	1420	7200	28	2165

The analysis was conducted with the use of FEM with an explicit integration method in the LS-Dyna software [4]. The tests were conducted for six different explosive materials and three different charge shapes, with varying length L to diameter D ratios and constant charge mass. In this study, the shapes with the L/D ratios of 2, 1 and 0.25 were used.

The applied model consisted of a 50 g explosive charge, surrounded by the air domain.

Charge was modelled by using the volume fraction geometry option in LS-Prepost (Fig. 2). The calculated domain model contained 3 791 760 hex finite elements.
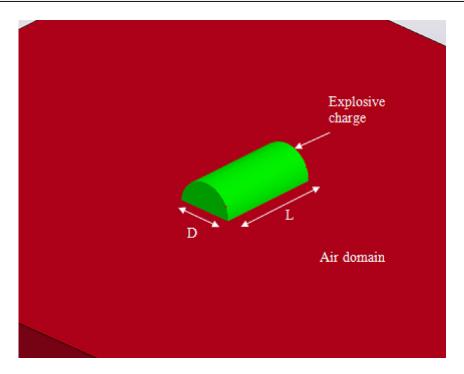
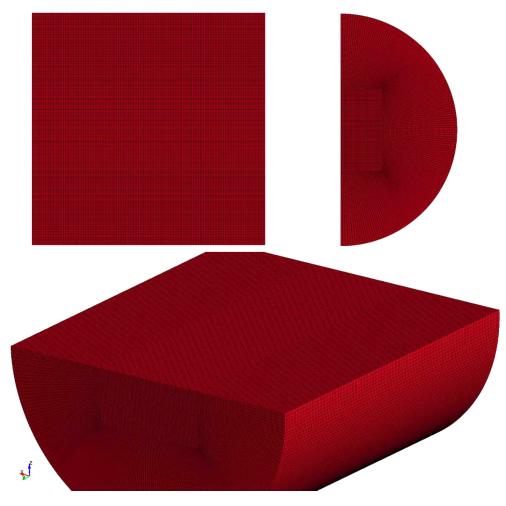**Fig. 1.** A numerical model of explosive charge.

Fig. 2. Model discretization.

3. ANALYSIS OF THE RESULTS

Figures 3–5 show the curves representing the blast waves caused by detonation of 50 g cylindrical charges for different explosive materials (Table 2). The pressure values are taken at a measuring point located at a distance of 35 cm from the centre along the axis of the explosive charge.
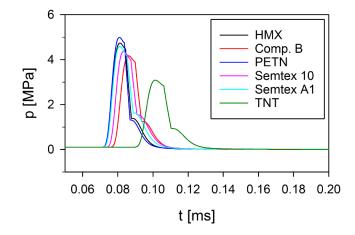
Fig. 3. Pressure values at a distance of 35 cm from centre for explosive charges with L/D = 0.25.
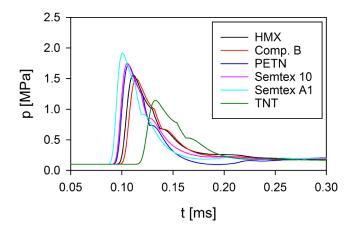
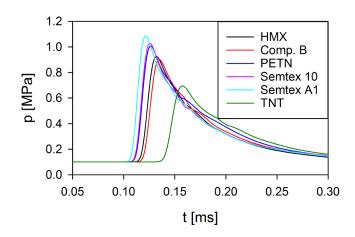**Fig. 4.** Pressure values at a distance of 35 cm from centre for explosive charges with L/D = 1.

Fig. 5. Pressure values at a distance of 35 cm from centre for explosive charges with L/D = 2.

Each curve represents an explosive material (i.e., HMX), grouped together in graphs by the L/D ratio. Figure 3 presents the results for the L/D ratio of 0.25 – a short, disc-shaped charge. Figure 4 presents the L/D ratio of 1, which is a charge closest to a spherical one in terms of overall dimensions. Figure 5 shows a longer, rod-like charge with L/D = 2.

Depending on the charge shape, significant differences between the blast waves as well as different pressure values were observed. The most significant differences were observed for the HMX charge, in which the pressure dropped from 4.74 MPa for L/D = 0.25 to 0.92 MPa for L/D = 2. The least significant differences were observed for the Semtex A1 charge, in which the pressure values dropped from 4.6 MPa to 1.1 MPa.

Contrary to expectations, the most typical curve course was observed for the charges with the L/D ratio of 2 (elongated), and not for the L/D ratio of 1 as anticipated (Fig. 5).

In the case where charges made of different explosive materials had the same L/D ratio, the course of the curves was similar, with only the TNT charge deviating from the rest. However, deviation in TNT was caused by the blast wave propagation velocity, and lower values of pressure and pressure impulse resulting from material properties, and not from the charge shape, as the overall shape of the curve is still similar to other curves.

The pressure impulse can be defined by:

$$I = \int\limits_{t_0}^{t_e} p(\tau)d\tau, \tag{3}$$

where $p(\tau)$ – blast wave course as a function of time, t_0 – pressure impulse start time, t_e – positive pressure impulse end time.

The differences would be even more significant if the charges were detonated from the side instead of the centre.

Differences in pressure impulse were observed in all propagation directions (Figs. 6–11). The elongated charges showed more significant differences (left sides of Figs. 6–11). The propagation of pressure impulse was the slowest at the angle of 45° in both cases, as it is evident from the isobars.

In every case, the most significant differences in pressure impulse appeared between the direction along the axis of the charge and the direction perpendicular to it.

The presented comparisons showed that no material exhibited increased susceptibility to the observed shape changes. Each of the resulting blast waves was characterized by a similar shape and course of pressure propagation. A change in charge shape itself influenced each explosive in a similar way, despite having a significant influence (resulting in higher pressure values, being even five times
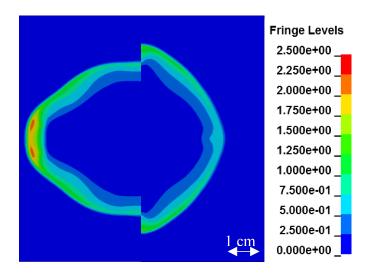

Fig. 6. Comparison of blast wave shapes for HMX charge with L/D equal to 0.25 (left) and 2 (right), 0.16 ms after detonation. Scale in MPa.
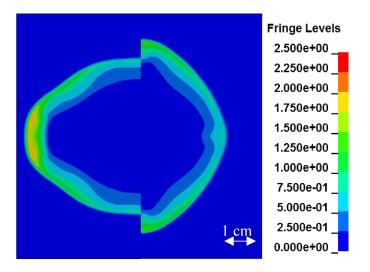
Fig. 7. Comparison of blast wave shapes for Semtex A1 charge with L/D equal to 0.25 (left) and 2 (right), 0.16 ms after detonation. Scale in MPa.
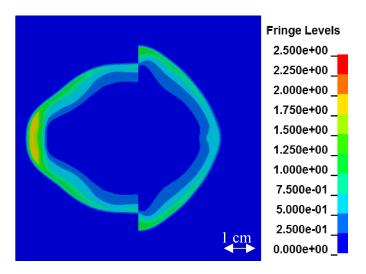

Fig. 8. Comparison of blast wave shapes for Comp B charge with L/D equal to 0.25 (left) and 2 (right), 0.16 ms after detonation. Scale in MPa.
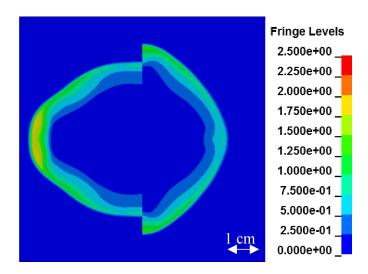

Fig. 9. Comparison of blast wave shapes for Semtex 10 charge with L/D equal to 0.25 (left) and 2 (right), 0.16 ms after detonation. Scale in MPa.
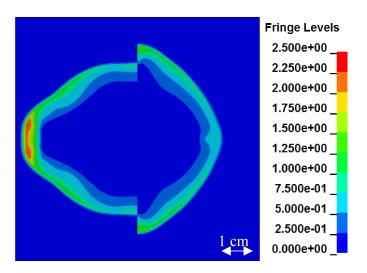
Fig. 10. Comparison of blast wave shapes for PETN charge with L/D equal to 0.25 (left) and 2 (right), 0.16 ms after detonation. Scale in MPa.
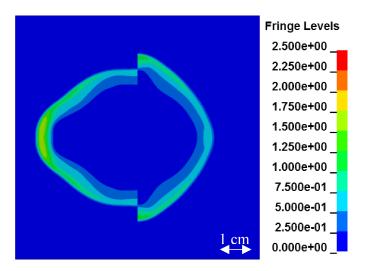

Fig. 11. Comparison of blast wave shapes for TNT charge with L/D equal to 0.25 (left) and 2 (right), 0.16 ms after detonation. Scale in MPa.

higher between the different ratios) on the overall character of the blast waves. The differences between each explosive resulted from different values of material properties. In particular, this was observed in TNT, which displayed much lower propagation velocity and pressure values while retaining its overall shape similar to other explosives.

4. CONCLUSION

In this study, we demonstrated that the blast waves generated by different explosive devices change their shapes in a predictable manner and each explosive exhibits a similar character of change. Although each explosive had different propagation velocity or pressure values, the overall course was always the same and changed in the same way while the charge geometry was modified. This was even the case for the explosive material properties exhibiting greater disparity in pressure or velocity values compared to other materials, which means that the charge shape is much more important than the explosive material itself. This is potentially significantly mitigating the differences resulting from the material properties. Therefore, it is important in experimental tests to take into consideration explosive charge shapes to avoid errors and disparities.

REFERENCES

[1] M.S. Chafi, G. Karami, M. Ziejewski. Numerical analysis of blast-induced wave propagation using FSI and ALE multi-material formulations. *International Journal of Impact Engineering*, **36**(10): 126–1275, 2009, DOI: 10.1016/j.ijimpeng.2009.03.007.

[2] R. Panowicz, J. Nowak, M. Konarzewski, T. Niezgoda. Introduction to numerical analysis of directed fragmentation warheads. *Journal of KONES Powertrain and Transport*, **20**(4): 319–325, 2013.

[3] E. Włodarczyk. *Introduction into Mechanics of Explosion* [in Polish: *Wstęp do mechaniki wybuchu*]. PWN, Warszawa, 1994.

[4] R. Panowicz, M. Konarzewski, J. Borkowski, E. Milewski. Selected aspects of modelling a phenomena occurring with very large strain rates on the example of the shaped charge jet stream forming process and explosive formed projectiles. *Journal of KONES*, **22**(3): 187–192, 2015, DOI: 10.5604/12314005.1166017.

[5] J.O. Hallquist. *LS-Dyna Theory Manual*. Livermore Software Technology Corporation.

[6] A. Alia, M. Souli. High explosive simulation using multi-material formulations. *Applied Thermal Engineering*, **26**(10): 103–1042, 2006.